Journal of Peptide Science
J. Peptide Sci. **9**: 203–211 (2003)
Published online in Wiley InterScience (www.interscience.wiley.com). DOI: 10.1002/psc.443

JOURNAL OF PEPTIDE SCIENCE

Synthesis and Conformational Characterization of Peptides Related to the Neck Domain of a Fungal Kinesin

DOMINGA DELUCA,[a†] GÜNTHER WOEHLKE[b] and LUIS MORODER[a*]

[a] Max-Planck-Institut für Biochemie, Am Klopferspitz 18a, 82152 Martinsried, Germany
[b] Adolf-Butenandt Institut, Zellbiologie, Ludwig-Maximilians-Universität München, Munich, Germany

Received 10 September 2002
Accepted 19 September 2002

Abstract: The Y362K mutation in the neck domain of conventional kinesin from *Neurospora crassa* provokes a significant reduction of the rate of movement along microtubules. Since the α-helical coiled-coil structure of the neck region is implicated in the mechanism of the processive movement of kinesins, a series of peptides related to the heptad region 338–379 of the wild-type and the variant fungal kinesins were synthesized as monomers and as *N*-terminal disulfide dimers, crosslinked to favour self-association into coiled-coil structures entropically. A comparison of the dichroic properties of the peptides and the effects of trifluoroethanol and peptide concentration clearly confirmed the strong implication of the single point mutation in destabilizing the intrinsic propensity of the peptides to fold into the supercoiled conformation. That there is a correlation between the stability of the coiled-coil and rate of movement of the kinesin is confirmed.

Keywords: kinesin peptides; neck region; synthesis; conformation; coiled-coil; circular dichroism

INTRODUCTION

Conventional kinesins are molecular motor proteins capable of transforming energy derived from ATP hydrolysis into movement [1,2]. They are thought to transport vesicles and organelles along the microtubules toward the microtubule plus end and thus from the centre to the periphery (anterograde transport) [3]. The *N*-terminal approximately 400 amino acid portion of conventional animal kinesins forms the so-called functional motor and is sufficient for wild-type motility behaviour. It forms the nucleotide- and microtubule-binding core motor domain ('head') and the neck region, whose relatively short coiled-coil structure is sufficiently stable to promote dimerization of the two heads [4–8]. A characteristic of the motion of conventional kinesins is its processivity; the protein 'walks' along microtubules in steps of 8 nm that correspond to the distance between two consecutive tubulin subunits [9]. In the course of this movement, the two heads alternate in function. While one head is bound to the filament in a nucleotide-free state, the other is loosely associated to the microtubule, but in a strong ADP-binding state [10]. The neck region apparently plays a crucial role in coordinating the interlaced reaction cycles of the two heads, as it is responsible for tethering the loosely microtubule-bound head to the filament, and may also be involved in guiding it to the next microtubule binding site. Possibly, a 'zipping' and 'unzipping' process of the neck coiled-coil structure allows the detached head to reach its next binding site, which is otherwise prevented for steric reasons [4,11,12].

Conventional fungal kinesins differ from those isolated from animals in lacking the light chains. Furthermore, fungal kinesins move approximately

* Correspondence to: Dr Luis Moroder, Max-Planck-Institut für Biochemie, Am Klopferspitz 18A, D-82152 Martinsried, Germany; e-mail: moroder@biochem.mpg.de
† Present address: Institute of Experimental Genetics, GSF-National Research Center for Environmental Health, 85764 Neuherberg, Germany.

three to five times faster (around 2.7 μm/s) than animal kinesins, and their ATP affinity is significantly lower [13–15]. In the neck coiled-coil region, the sequence composition of conventional fungal kinesin predicts a greater coiled-coil propensity than the neck region of conventional animal kinesins. As the neck region plays a crucial role in the process of movement, a more stable coiled-coil conformation could somehow be correlated to a higher rate of movement [15]. Replacement of Tyr-362 in the neck coiled-coil region of *Neurospora crassa* kinesin by Lys ($Nkin_{Y362K}$), the residue present in the analogous position in the *Drosophila melanogaster* kinesin, caused a significant acceleration of the steady state ATPase ($k_{cat} = 262\ s^{-1}$ vs $72\ s^{-1}$), but a strong decrease of the gliding velocity (1.1 ± 0.2 μm/s vs 2.6 μm/s for the wild-type) [16]. This effect provoked by the single mutation may be attributable to conformational changes in the neck region, i.e. in the two-stranded α-helical coiled-coil.

In coiled-coil structures, two or more helices interact with each other forming a super coil. This structural motif is characterized by heptad repeats $(a\text{-}b\text{-}c\text{-}d\text{-}e\text{-}f\text{-}g)_n$ where the positions *a* and *d* are predominantly occupied by hydrophobic residues [17,18]. The interhelical hydrophobic interactions between amino acids present in positions *a* and *d* are essential in stabilizing, as well as holding together, the whole coiled-coil. The positions *e* and *g*, if occupied by side-chain charged amino acids, can be involved in ionic interactions with each other, although the role of such salt bridges is not always decisive for the stability of this structure [19,20]. In the case of *N. crassa* kinesin, Tyr-362 is located in position *g* of the heptad at the edge of the hydrophobic core, while in the Y362K variant this position is occupied by a Lys residue, which could form a salt bridge with Glu-367 in position *e*, and thus stabilize the coiled-coil structure.

The aim of the present study was to analyse the conformational preferences of peptides related to the neck region of *N. crassa* kinesin, in order to prove or disprove the effect of the Y362K mutation on coiled-coil propensities (and thus on the possibly correlated rates of movement). For this purpose peptides corresponding to the neck domain and comprising the sequence 338–379 (Kn1) of the wild-type kinesin (Kn1) as well as of the variant Y362K (Kn2) were synthesized (Figure 1). This sequence exceeds the expected coiled-coil by five amino acid residues at both the *N*- and *C*-termini. To favour the onset of the coiled-coil structure entropically, a second set of peptides (Kn3 and Kn4) was synthesized in

Figure 1 Peptides related to sequences of the fungal conventional kinesin neck domain from *Neurospora crassa* and the related Y362K variant.

which the Pro residue in position *a* of the first heptad was replaced by a cysteine, since disulfide crossbridging into dimers in this position is known not to affect sterically a supercoiling of the dimers [17,21]. Moreover, the peptides were shortened *C*-terminally to facilitate the synthesis (Kn5 and Kn6).

EXPERIMENTAL

Materials and Methods

All reagents and solvents used were of the highest quality commercially available. Amino acid derivatives were from Alexis (Grünberg, Germany) or were prepared according to standard protocols. TentaGel-S-PHB resin (loading 0.25 mmol/g) and MBHA resin (loading: 1.2 mmol/g) were used as solid supports. Analytical RP-HPLC was carried out on ET 125/4 Nucleosil 100-5 C_8 columns (Macherey & Nagel, Düren, Germany) by elution with a linear gradient of MeCN2% H_3PO_4 from 5 : 95 to 80 : 20 in 12 min at a flow rate of 1.5 ml/min and monitoring at 210 nm. Amino acid analyses of the acid hydrolysates (6 M HCl containing 2.5% thioglycolic acid, 110 °C, 24 h) were performed on a LC 6001 Biotronic amino acid analyser.

Synthesis of Kn1 and Kn2

The peptides were synthesized on TentaGel S RAM resin on an automated Applied Biosystem model 431A peptide synthesizer by Fmoc chemistry using *tert*-butanol based side-chain protection. Double coupling was applied in each acylation step with Fmoc-amino acid/HBTU/HOBt/DIPEA (4 : 4 : 4 : 8 equiv) (2 × 30 min) in DMF/CH_2Cl_2 (8 : 2). Fmoc cleavage was performed with 20% piperidine in NMP (1 × 3 min and 1 × 15 min). The *N*-terminal acetylation was carried out with Ac_2O/DIPEA (10 : 15 equiv) in DMF (2 × 40 min) and deprotection/resin cleavage with TFA/H_2O/triisopropylsilane (95 : 10 : 1.5) in 90 min. The resin was filtered off and washed with the cleavage cocktail; the filtrates were combined and taken to dryness. The crude products were precipitated from MeOH with diisopropyl ether, dissolved in 50 mM AcOH and lyophilized. Purification of the crude products was carried out by RP-HPLC using a Nucleosil® C18 column (Macherey & Nagel, Düren, Germany) and as eluent a linear gradient of 0.1% TFA in water and 0.08% TFA in MeCN at a flow rate of 9 ml/min. Fractions containing the desired material were pooled and lyophilized to constant weight.

Ac-Ala-Glu-Leu-Ser-Pro-Ala-Glu-Leu-Lys-Gln-Met-Leu-Ala-Lys-Ala-Lys-Thr-Gln-Ile-Thr-Ser-Phe-Glu-Asn-Tyr-Ile-Val-Asn-Leu-Glu-Ser-Glu-Val-Gln-Val-Trp-Arg-Gly-Gly-Glu-Thr-Val-NH_2 (Kn1). Overall yield: 6%; HPLC: $t_R = 9.7$ min; ESI-MS: $m/z = 2376.0$ $[M + 2H]^{2+}$, 1584.2 $[M + 3H]^{3+}$, 1188.4 $[M + 4H]^{4+}$; $M_r = 4750.4$ calcd for $C_{211}H_{339}N_{55}O_{67}S$; amino acid analysis: Asp 2.08 (2), Thr 3.33 (3), Ser 2.87 (3), Glu 8.88 (9), Pro 1.00 (1), Gly 2.07 (2), Ala 3.59 (4), Val 3.83 (4), Met 0.94 (1), Ile 1.75 (2), Leu 3.71 (4), Tyr 0.95 (1), Phe 1.14 (1), Lys 2.75 (3), Trp 0.96 (1), Arg 1.00 (1): peptide content: 70.8%.

Ac-Ala-Glu-Leu-Ser-Pro-Ala-Glu-Leu-Lys-Gln-Met-Leu-Ala-Lys-Ala-Lys-Thr-Gln-Ile-Thr-Ser-Phe-Glu-Asn-Lys-Ile-Val-Asn-Leu-Glu-Ser-Glu-Val-Gln-Val-Trp-Arg-Gly-Gly-Glu-Thr-Val-NH_2 (Kn2). Overall yield: 4%; HPLC: $t_R = 9.4$ min; ESI-MS: $m/z = 2358.4$ $[M + 2H]^{2+}$, 1572.8 $[M + 3H]^{3+}$, 1179.8 $[M + 4H]^{4+}$, 944.2 $[M + 5H]^{5+}$; $M_r = 4715.4$ calcd for $C_{208}H_{342}N_{56}O_{66}S$; amino acid analysis: Asp 1.94 (2), Thr 3.04 (3), Ser 2.86 (3), Glu 8.10 (9), Gly 1.95 (2), Ala 3.51 (4), Val 3.43 (4), Met 0.95 (1), Ile 1.68 (2), Leu 4.05 (4), Phe 1.00 (1), Lys 3.95 (4), Trp 1.04 (1), Arg 1.07 (1); peptide content: 75.1%.

Synthesis of Kn3, Kn4, Kn5 and Kn6

The peptides were synthesized manually on MBHA resin by Boc chemistry, using for side-chain protection Lys[Z(2-Cl)], Glu(cHxl), Tyr[Bzl(2-Br)], Arg(Tos) in addition to benzyl ethers and esters. Despite the acid lability of *S*-Mob protection, Cys(Mob) was used, as this residue is introduced in the penultimate acylation step and thus exposed to acid treatment only once before the final deprotection. Couplings were generally performed with Boc-amino acid/DCC (2 : 2 equiv) in CH_2Cl_2 (1.5 h), except for Boc-Gln(Trt)-OH, Boc-Asn(Trt)-OH and Boc-Arg(Tos)-OH which were coupled with Boc-amino acid/DCC/HOBt (2 : 2 : 3 equiv) in DMF (1.5 h). When double couplings (were required according to the Kaiser test [22]), coupling was repeated with 1 to 2 equiv Boc-amino acid/TBTU/DIPEA (1 : 1 : 2.5) in DMF for 1.5 h. If required, capping was performed with 20% Ac_2O in CH_2Cl_2 for 15 min. After each coupling and capping step the resin was washed with MeOH (2 × 3 min) and CH_2Cl_2 (2 × 3 min) or with DMF (1 × 3 min), MeOH (2 × 3 min) and CH_2Cl_2 (2 × 3 min) when

DMF was used as solvent in the acylation reaction. Boc cleavage was carried out with 60% TFA in CH_2Cl_2 containing 0.5% anisole (30 min), then the resin was washed with CH_2Cl_2 (2×3 min), isopropanol (2×3 min), 10% TEA in CH_2Cl_2 (1×1 min and 1×9 min), CH_2Cl_2 (1×5 min), MeOH (2×3 min) and CH_2Cl_2 (2×3 min). For deprotection/resin cleavage the resin was treated with liquid HF (6.0 ml/g resin) containing 10% anisole for 75 min at 0 °C. The resin was washed several times with cold MTB and extracted several times with 5% AcOH. The extracts were combined and lyophilized. The crude products were purified by RP-HPLC on a preparative PrepPak® C18 column using as eluent a linear gradient of 0.1% TFA in water and 0.1% TFA in MeCN at a flow rate of 100 ml/min. Fractions containing the desired product were pooled and lyophilized.

H-Ser-Cys-Ala-Glu-Leu-Lys-Gln-Met-Leu-Ala-Lys-Ala-Lys-Thr-Gln-Ile-Thr-Ser-Phe-Glu-Asn-Tyr-Ile-Val-Asn-Leu-Glu-Ser-Glu-Val-Gln-Val-Trp-Arg-Gly-Gly-Glu-Thr-Val-NH_2 (Kn3 monomer). Overall yield: 0.7%; HPLC: $t_R = 9.16$ min and a minor contamination at $t_R = 8.7$ min (dimer); ESI-MS: $m/z = 2200.6$ $[M + 2H]^{2+}$, 1468.0 $[M + 3H]^{3+}$, 1101.0 $[M + 4H]^{4+}$, 881.2 $[M + 5H]^{5+}$; $M_r = 4401.3$ calcd for $C_{193}H_{313}N_{52}O_{61}S_2$.

H-Ser-Cys-Ala-Glu-Leu-Lys-Gln-Met-Leu-Ala-Lys-Ala-Lys-Thr-Gln-Ile-Thr-Ser-Phe-Glu-Asn-Lys-Ile-Val-Asn-Leu-Glu-Ser-Glu-Val-Gln-Val-Trp-Arg-Gly-Gly-Glu-Thr-Val-NH_2 (Kn4 monomer). Overall yield: 1.5%; HPLC: $t_R = 8.78$ min and minor contamination at $t_R = 8.85$ min (dimer); ESI-MS: $m/z = 2183.8$ $[M + 2H]^{2+}$, 1456.4 $[M + 3H]^{3+}$, 1092.4 $[M + 4H]^{4+}$; $M_r = 4366.3$ calcd for $C_{190}H_{315}N_{53}O_{60}S_2$.

H-Ser-Cys-Ala-Glu-Leu-Lys-Gln-Met-Leu-Ala-Lys-Ala-Lys-Thr-Gln-Ile-Thr-Ser-Phe-Glu-Asn-Tyr-Ile-Val-Asn-Leu-Glu-Ser-Glu-Val-Gln-Val-NH_2 (Kn5 monomer). Overall yield: 4%; HPLC: $t_R = 9.19$ min; ESI-MS: $m/z = 1808.4$ $[M + 2H]^{2+}$, 1205.8 $[M + 3H]^{3+}$, 904.6 $[M + 4H]^{4+}$; $M_r = 3615.4$ calcd for $C_{158}H_{261}N_{41}O_{51}S_2$.

H-Ser-Cys-Ala-Glu-Lys-Gln-Met-Leu-Ala-Lys-Ala-Lys-Thr-Gln-Ile-Thr-Ser-Phe-Glu-Asn-Lys-Ile-Val-Asn-Leu-Glu-Ser-Glu-Val-Gln-Val-NH_2 (Kn6 monomer). Overall yield: 3%; HPLC: $t_R = 8.67$ min; ESI-MS: $m/z = 1791.0$ $[M + 2H]^{2+}$, 1194.4 $[M + 3H]^{3+}$, 896.0 $[M + 4H]^{4+}$; $M_r = 3580.4$ calcd for $C_{155}H_{264}N_{42}O_{50}S_2$.

The monomeric monocysteine peptides were oxidized to homodimers at about 1 mg/0.2 ml water concentration by gentle stirring overnight under air oxygen. The progress of the reaction was monitored by HPLC and Grassetti test [23]. The products were isolated as lyophilizates.

(H-Ser-Cys-Ala-Glu-Leu-Lys-Gln-Met-Leu-Ala-Lys-Ala-Lys-Thr-Gln-Ile-Thr-Ser-Phe-Glu-Asn-Tyr-Ile-Val-Asn-Leu-Glu-Ser-Glu-Val-Gln-Val-Trp-Arg-Gly-Gly-Glu-Thr-Val-NH_2)$_2$ (Kn3). HPLC: $t_R = 11.15$ min at 45 °C; ESI-MS: $m/z = 2201.2$ $[M + 4H]^{4+}$, 1761.2 $[M + 5H]^{5+}$, 1467.6 $[M + 6H]^{6+}$, 1258.0 $[M + 7H]^{7+}$, 1101.0 $[M + 8H]^{8+}$, 978.8 $[M + 9H]^{9+}$; $M_r = 8800.6$ calcd for $C_{386}H_{624}N_{104}O_{122}S_4$; amino acid analysis: Asp 3.88 (4), Thr 5.61 (6), Ser 5.10 (6), Glu 14.09 (14), Gly 3.99 (4), Ala 5.06 (6), Cys 2.01 (2), Val 7.67 (8), Met 1.70 (2), Ile 3.34 (4), Leu 5.36 (6), Tyr 1.85 (2), Phe 1.94 (2), Lys 4.96 (6), Trp 1.50 (2), Arg 2.00 (2); peptide content: 87.5%.

(H-Ser-Cys-Ala-Glu-Leu-Lys-Gln-Met-Leu-Ala-Lys-Ala-Lys-Thr-Gln-Ile-Thr-Ser-Phe-Glu-Asn-Lys-Ile-Val-Asn-Leu-Glu-Ser-Glu-Val-Gln-Val-Trp-Arg-Gly-Gly-Glu-Thr-Val-NH_2)$_2$ (Kn4). HPLC: $t_R = 10.79$ min at 35 °C; ESI-MS: $m/z = 1747.2$ $[M + 5H]^{5+}$, 1456.0 $[M + 6H]^{6+}$, 1248.0 $[M + 7H]^{7+}$, 1092.4 $[M + 8H]^{8+}$, 971.0 $[M + 9H]^{9+}$; $M_r = 8730.6$ calcd for $C_{380}H_{628}N_{106}O_{120}S_4$; amino acid analysis: Asp 4.22 (4), Thr 5.88 (6), Ser 5.29 (6), Glu 15.21 (16), Gly 4.37 (4), Ala 5.56 (6), Cys 1.16 (2), Val 7.92 (8), Met 1.80 (2), Ile 5.83 (6), Phe 2.00 (2), Lys 7.28 (8), Trp 1.91 (2), Arg 2.40 (2); peptide content: 79.8%.

(H-Ser-Cys-Ala-Glu-Leu-Lys-Gln-Met-Leu-Ala-Lys-Ala-Lys-Thr-Gln-Ile-Thr-Ser-Phe-Glu-Asn-Tyr-Ile-Val-Asn-Leu-Glu-Ser-Glu-Val-Gln-Val-NH_2)$_2$ (Kn5). HPLC: $t_R = 9.55$ min; ESI-MS: $m/z = 1808.2$ $[M + 4H]^{4+}$, 1446.6 $[M + 5H]^{5+}$, 1206.0 $[D + 6H]^{6+}$; $M_r = 7228.8$ calcd for $C_{316}H_{520}N_{82}O_{102}S_4$; amino acid analysis: Asp 4.00 (4), Thr 3.88 (4), Ser 5.15 (6), Glu 13.84 (14), Ala 5.52 (6), Val 5.48 (6), Met 1.86 (2), Ile 3.56 (4), Leu 6.25 (6), Tyr 2.09 (2), Phe 1.99 (2), Lys 5.64 (6); peptide content: 78.7%.

(H-Ser-Cys-Ala-Glu-Lys-Gln-Met-Leu-Ala-Lys-Ala-Lys-Thr-Gln-Ile-Thr-Ser-Phe-Glu-Asn-Lys-Ile-Val-Asn-Leu-Glu-Ser-Glu-Val-Gln-Val-NH_2)$_2$ (Kn6). HPLC: $t_R = 9.25$ min; ESI-MS: $m/z = 1790.8$ $[M + 4H]^{4+}$, 1432.6 $[D + 5H]^{5+}$, 1194.0 $[M + 6H]^{6+}$, 1023.8 $[M + 7H]^{7+}$, 896.0 $[M + 8H]^{8+}$, 796.2 $[D + 9H]^{9+}$, 717.0 $[D + 10H]^{10+}$; $M_r = 7158.8$ calcd for $C_{310}H_{526}N_{84}O_{100}S_4$; amino acid analysis: Asp 4.00

(4), Thr 3.94 (4), Ser 5.83 (6), Glu 13.47 (14), Ala 6.77 (6), Cys 1.82 (2), Val 5.37 (6), Met 1.93 (2), Ile 3.04 (4), Leu 6.24 (6), Phe 2.15 (2), Lys 7.41 (8); peptide content: 69.4%.

Circular Dichroism

The CD spectra were recorded on a Jasco J-715 spectropolarimeter equipped with a thermostated cell holder and connected to a data station for signal averaging and processing. All spectra were recorded in the range 190–250 nm with a scanning speed of 50 nm/min, a response of 1 s and a band width of 1.0 nm, at 20 °C in quartz cuvettes of 0.1 cm optical path length. The collected spectra (average of 10 scans) were all normalized and the ellipticity expressed as mean residue molar ellipticity $[\Theta]_R$ (deg cm^2 dmol^{-1}). For sample preparation each solution was filtered through membrane filters (0.45 μm) and the concentration was determined by UV absorbance at 280 nm based on the absorption coefficients of Tyr and Trp, and in the absence of these chromophores by weight and peptide content as determined by quantitative amino acid analysis. The UV spectra were taken on an UV/VIS spectrometer Lambda 19 of Perkin Elmer. If not stated otherwise, the CD spectra were recorded in 50 mM phosphate buffer at the indicated pH and at 20 °C. The CD spectra of the peptides Kn1 and Kn2 at different concentrations were recorded with cuvettes of a path length of 0.01 cm, 0.1 cm and 1 cm.

The melting curves were measured by following the change of the molar ellipticity at 222 nm in function of temperature with a temperature slope of 30 °C/h, the response of 16 s and the band width of 1 nm. The temperature at the zero point of the second derivative of the relative melting curve was taken as melting temperature (T_m).

Mass Spectrometry

Mass spectra were measured on a PE SCIEX API 165 single quadrupole MS system. The spectra for detecting the non-covalently bound dimers were taken in the range 700–2000 Da, with an infusion pump rate of 0.3 ml/h, an ion source high voltage of 4.5 kV, an orifice voltage of 15V, a dwell time of 0.6 ms per scan and a step size of 0.2 Da with 10 scans summed.

RESULTS

Peptide Synthesis

To better mimic the peptides of the neck coiled-coil region of *Neurospora crassa* kinesin as integral fragments of the proteins and particularly to prevent unfavourable electrostatic interactions between helices in a coiled-coil conformation [17,24] Kn1 and Kn2 (Figure 1) were *N*-acetylated and *C*-amidated, while the *N*-terminally disulfide crosslinked Kn3–Kn6 peptides were not N^{α} -acetylated to possibly facilitate purification and enhance the solubility. In fact, in the synthesis of this series of peptides difficulties were encountered in the assembly on resin as well assessed by the continuous need of double couplings and by the complete failure in the synthesis of Kn5 by the Fmoc chemistry. The sequence was purposely shortened at the *C*-terminus to facilitate the synthesis, but the opposite effect was observed. Therefore only the Kn1 and Kn2 were accessible by the Fmoc chemistry at a degree of purity of the crude products that allowed their isolation as homogeneous materials by RP-HPLC adopting a very slow gradient, although at very low yields. Boc chemistry was chosen for the synthesis of Kn3, Kn4, Kn5 and Kn6, since this strategy is well known to yield better results with difficult sequences because of the repetitive acidic TFA treatments. However, particularly in the case of the peptides Kn5 and Kn6, very careful monitoring of each coupling step and capping with Ac_2O was required, even using this strategy. Again the low yields reflect the difficulty of obtaining these molecules as well characterized compounds and at a degree of purity that serves for a careful examination of the their conformational preferences.

Conformational Properties of the Monomeric Kinesin Peptides Kn1 and Kn2

Circular dichroism. In a previous communication we have reported and discussed the dichroic properties of the wild-type Kn1 peptide [25]. Similarly to Kn1 the CD spectra of Kn2 corresponding to the Y362K variant sequence, also show a clear pH dependence and are supportive of significant helical structure at pH 3, whereas at higher pH values a tendency to aggregation is noted (Figure 2). Although the spectrum of the variant at pH 3 and 20 °C is consistent with an α-helical conformation, in contrast to the wild-type Kn1 a coiled-coil has to be

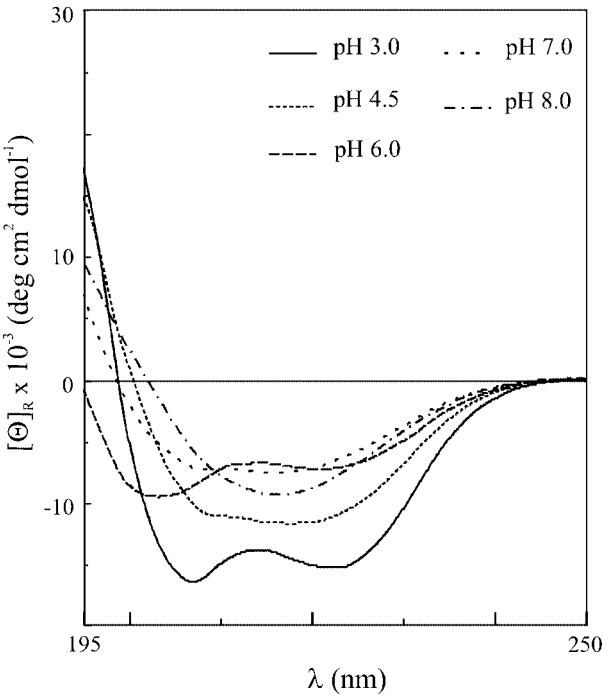

Figure 2 CD spectra of Kn2 in 50 mM phosphate buffer at increasing pH values.

excluded because of the low value of the $[\Theta]_{222}/[\Theta]_{208}$ ratio (<1) [17,18,24].

TFE is known to stabilize secondary structures such as helices, but at the same time to destabilize tertiary folds such as coiled-coils [26,27]. Increasing the content of TFE in the Kn2 solution at pH 3 from 0 to 70% causes an increase of the α-helical structure (data not shown), but the ratio $[\Theta]_{222}/[\Theta]_{208}$ remains <1 as additional evidence for the absence of coiled-coil at 20°C. The formation of a two-stranded α-helical coiled-coil is a bimolecular process and the monomer/dimer equilibrium is thus affected by the peptide concentration [18]. For Kn1 the helical content increases with the peptide concentration reaching a plateau value at about 10^{-5} M (Figure 3) where a maximum of ordered structure is reached. In the case of Kn2 such concentration-dependent helical content is also observed, but a plateau value is not reached. At 10^{-3} M concentrations both peptides display a great tendency to aggregation.

Thermal denaturation of both Kn1 and Kn2 was monitored at 222 nm in the 5° to 70°C temperature range. A cooperative transition with a T_m of 47.2°C was obtained for Kn1 which was accompanied by a concurrent decrease of the coiled-coil structure [25]. The CD spectra of Kn2 at pH 3 monitored at increasing temperatures are characterized by an

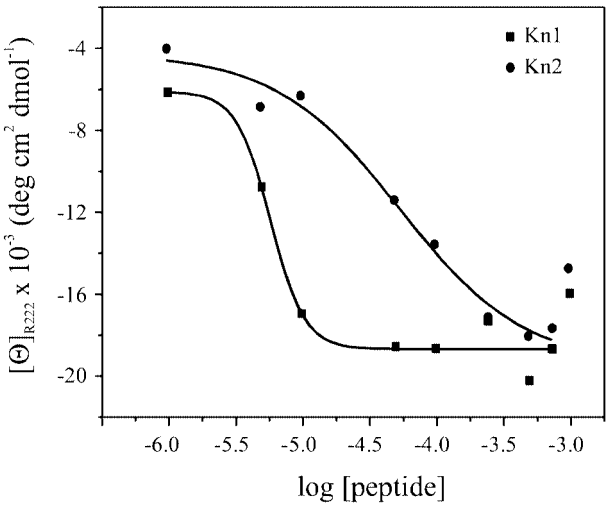

Figure 3 Concentration dependency of the dichroic intensities at 222 nm of the Kn1 and Kn2 peptides.

isodichroic point at 203 nm which is supportive of a two-state transition from a folded to unfolded form. Moreover, at 5°C a $[\Theta]_{222}/[\Theta]_{208}$ ratio of 1.07 was determined that clearly confirms that even Kn2 is capable of assuming the coiled-coil conformation at least at low temperature. Compared with Kn1, the folded state of Kn2 is significantly less stable (T_m = 19.6°C) and thermal denaturation leads to aggregation, thus making the process irreversible.

Mass spectrometry. The presence of a coiled-coil conformation in solution implies that the peptides form dimers linked by non-covalent bonds. An indirect mode of proving such conformation in solution consists in the detection of dimers. Among the various techniques that allow identification of non-covalent complexes, ESI-MS has been shown to be very useful [28,29]. Therefore mass spectra were recorded for Kn1 and Kn2 in aqueous AcOH (pH 3) where CD spectra were almost identical to those recorded in phosphate buffer at pH 3.0. For Kn1 the presence of peaks corresponding to the dimer ions $[M + 5H]^{5+}$ and $[M + 7H]^{7+}$ confirm that this peptide folds as a two-stranded α-helical coiled-coil at pH 3. For Kn2 only a peak of low intensity and corresponding to the dimer ion $[M + 5H]^{5+}$ was detected confirming the lower propensity of this Y364K variant to adopt the coiled-coil conformation.

Conformational Properties of the Dimeric Kinesin Peptides Kn3–Kn6

The CD spectra of the dimeric peptides (Kn3–Kn6) at different pH values are significantly different from

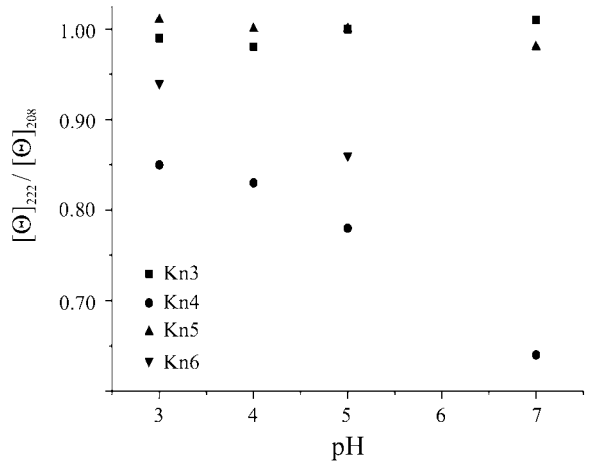

Figure 4 Variation of the $[\Theta]_{222}/[\Theta]_{208}$ ratios with pH for the peptides Kn3, Kn4, Kn5 and Kn6.

those of the monomeric Kn1 and Kn2 (Figure 4). While Kn3 and Kn5 display a propensity to fold as a two-stranded α-helical coiled-coil in the whole pH range investigated, the conformation of Kn4 and Kn6 is pH dependent, and an increase of the pH is associated with a decrease of the helical content and solubility.

Thermal denaturation was recorded at pH 3 and at pH 5. At 5 °C the $[\Theta]_{222}/[\Theta]_{208}$ ratios of Kn3 and Kn5 are clearly >1, supporting the coiled-coil conformation. A plot of the ratios vs temperature at both pH values reveals two transitions. The first, corresponding to dissociation of the supercoil into the α-helix, is a continuous monotonous process whereas the second transition is cooperative and thus related to unfolding of the α-helix and formation of aggregates (Figure 5). At pH 3 the T_m corresponding to the transition α-helix/aggregates is higher than that at pH 5, because of the higher helix stability under more acidic conditions. For the dimeric Kn4 and Kn6, the melting process involves only unfolding of the helix, while aggregation is not so significant compared with the wild type peptides.

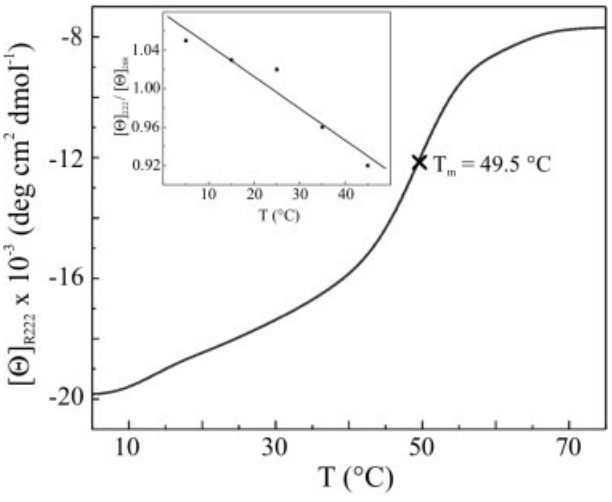

Figure 5 Thermal denaturation of Kn3 in 50 mM phosphate buffer (pH 3.0); insert: plot of $[\Theta]_{222}/[\Theta]_{208}$ *vs* temperature.

DISCUSSION

The conventional kinesin neck region is folded into a two-stranded α-helical coiled-coil which is believed to play a key role in the mechanism of movement. Since the variant $Nkin_{Y362K}$ of *N. crassa* kinesin displays a significantly lower rate of movement than the wild-type motor domain, this single mutation in the neck region has to provoke structural changes that decrease rates of movement.

In contrast to the prediction algorithms, a comparison of the dichroic properties of monomeric Kn1 and its Y364K variant (Kn2) indicates that the mutation reduces the propensity for self-association into the supercoiled structure, particularly at acidic pH values. At neutral pH both peptides tend to aggregate. This phenomenon of aggregation was not observed with peptides related to the homologous neck region of the human kinesin where the coiled-coil fold was detected at pH 7 [4,8]. A stabilization of the supercoil under acidic conditions has been reported and explained with the positive effects of protonated glutamic acid residues which display greater helical propensity and higher hydrophobicity, thus enhancing the hydrophobic surface and correspondingly, the contact area between the helices if located in position *e* or *g* of the heptad repeat [19,20]. In the peptides analysed in the present study two Glu residues are located in the position *e* of the heptades. By disulfide crosslinking of the peptides entropically to favour the supercoil, the effect of the Y362K mutation becomes even more evident. In fact, the wild-type dimeric fragment is folded as coiled-coil in the pH range between 3 and 7, while for the dimeric Y362K variant the supercoil can be excluded and the α-helical conformation decreases with increasing pH values. These results indicate that a salt bridge between Lys-362 and Glu-367 as promoted in the variant does not stabilize the coiled-coil conformation, whereas the protonated

side chain of Glu apparently provides a greater contribution in this context in agreement with previous studies [19,20,30].

In summary, the present study demonstrates that peptides derived from fungal kinesin's wild-type neck domain have a higher coiled-coil propensity than those based on the $Nkin_{Y362K}$ variant. These data agree with the observation that the $Nkin_{Y362K}$ mutants in constructs comprising the sequence portions 1–391 or 1–433 are monomeric, while their corresponding wild-type counterparts form dimers [16]. These motor-protein mutants seem to uncouple ATP hydrolysis and stepping because of the absence of two coordinated motor heads. Apparently, a rate-limiting step of the ATPase cycle is connected to the presence of a second head which is connected via the neck domain. Surprisingly, the Y362K mutation seems to exert an additional effect in the protein context that is unrelated to the dimerization behaviour. In fact, by comparing a monomeric Nkin variant (Nkin383) with the Y362K point mutant in the same background a 6- to 7-fold higher ATPase activity of the mutant was still observed [16]. Thus, the neck Tyr residue conserved in fungal conventional kinesins may fulfil a dual physiological function, i.e. stabilize the neck coiled-coil structure in an active dimeric motor, and down-regulate the activity in a repressed state, probably in a non-supercoiled neck conformation.

Acknowledgements

The authors are grateful to Dr W. Heinzel, PolyPeptide Laboratories GmbH, Wolfenbüttel, Germany, for offering his facilities to perform the synthesis with the Boc chemistry.

REFERENCES

1. Vale RD, Milligan RA. The way things move: looking under the hood of molecular motor proteins. *Science* 2000; **288**: 88–95.
2. Vale RD. Millennial musing on molecular motors. Millennium issue *TCB-TIBS-TIG* 1999; M38–M42.
3. Sack S, Kull FJ, Mandelkow E. Motor proteins of the kinesin family. *Eur. J. Biochem.* 1999; **262**: 1–11.
4. Tripet B, Vale RD, Hodges RS. Demonstration of coiled-coil interactions within the kinesin neck region using synthetic peptides. *J. Biol. Chem.* 1997; **272**: 8946–8956.
5. Kozielski F, Sack S, Marx A, Thormaehlen M, Schoenbrunn E, Biou V, Thompson A, Mandelkow E-M, Mandelkow E. The crystal structure of dimeric kinesin and implications for microtubule-dependent motility. *Cell* 1997; **91**: 985–994.
6. Huang T-G, Suhan J, Hackney DD. Drosophila kinesin motor domain extending to amino acid position 392 is dimeric when expressed in *Escherichia coli*. *J. Biol. Chem.* 1994; **269**: 16 502–16 507.
7. Thormaehlen M, Marx A, Sack S, Mandelkow E. The coiled-coil helix in the neck of kinesin. *J. Struct. Biol.* 1998; **122**: 30–41.
8. Morii H, Takenawa T, Arisaka F, Shimizu T. Identification of kinesin neck region as a stable α-helical coiled-coil and its thermodynamic characterization. *Biochemistry* 1997; **36**: 1933–1942.
9. Hancock WO, Howard J. Processivity of the motor protein kinesin requires two heads. *J. Cell Biol.* 1998; **140**: 1395–1405.
10. Hackney DD. Highly processive microtubule-stimulated ATP hydrolysis by dimeric kinesin head domains. *Nature* 1995; **377**: 448–450.
11. Sablin EP. Kinesins and microtubules: their structures and motor mechanisms. *Curr. Opin. Cell Biol.* 2000; **12**: 35–41.
12. Woehlke G, Schliwa M. Directional motility of kinesin motor proteins. *Biochim. Biophys. Acta* 2000; **1496**: 117–127.
13. Steinberg G, Schliwa M. Characterization of the biophysical and motility properties of kinesin from the fungus *Neurospora crassa*. *J. Biol. Chem.* 1996; **271**: 7516–7521.
14. Grummt M, Pistor S, Lottspeich F, Schliwa M. Cloning and functional expression of a 'fast' fungal kinesin. *FEBS Lett.* 1998; **427**: 79–84.
15. Kirchner J, Woehlke G, Schliwa M. Universal and unique features of kinesin motors: insights from a comparison of fungal and animal conventional kinesins. *Biol. Chem.* 1999; **380**: 915–921.
16. Schäfer F, Deluca D, Majdic U, Kirchner J, Schliwa M, Moroder L, Woehlke G. A conserved tyrosine in the neck of a fungal kinesin regulates the catalytic motor core. *EMBO J.* 2002; **22**: 450–458.
17. Hodges RS. *De novo* design of α-helical proteins: basic research to medical applications. *Biochem. Cell Biol.* 1996; **74**: 133–154.
18. Zhou NE, Zhu B-Y, Kay CM, Hodges RS. The two-stranded α-helical coiled-coil is an ideal model for studying protein stability and subunit interactions. *Biopolymers* 1992; **32**: 419–426.
19. Kohn WD, Kay CM, Hodges RS. Protein destabilization by electrostatic repulsions in the two-stranded α-helical coiled-coil/leucine zipper. *Protein Sci.* 1995; **4**: 237–250.
20. Kohn WD, Kay CM, Hodges RS. Orientation, positional, additivity, and oligomerization-state effect of interhelical ion pairs in α-helical coiled-coils. *J. Biol. Chem.* 1998; **283**: 993–1012.

21. Zhou NE, Kay CM, Hodges RS. Disulfide bond contribution to stability: positional effects of substitution in the hydrophobic core of the two-stranded α-helical coiled-coil. *Biochemistry* 1993; **32**: 3178–3187.
22. Kaiser E, Colescott RL, Bossinger CD, Cook PI. Colour test for the detection of free terminal amino groups in the solid-phase synthesis of peptides. *Anal. Biochem.* 1970; **34**: 595–598.
23. Grassetti DR, Murray JF Jr. Determination of sulfhydryl groups with 2,2′- or 4,4′- dithiodipyridine. *Arch. Biochem. Biophys.* 1967; **119**: 41–49.
24. Su JY, Hodges RS, Kay CM. Effect of chain length on the formation and stability of synthetic α-helical coiled-coils. *Biochemistry* 1994; **33**: 15 501–15 510.
25. Kallipolitou A, Deluca D, Majdic U, Lakämper S, Cross R, Mayhöfer E, Moroder L, Schliwa M, Woehlke G. Unusual properties of the fungal conventional kinesin neck domain from *Neurospora crassa*. *EMBO J.* 2001; **20**: 6226–6235.
26. Soennichsen FD, Van Eyk JE, Hodges RS, Sykes BD. Effect of trifluoroethanol on protein secondary structure: An NMR and CD study using a synthetic actin peptide. *Biochemistry* 1992; **31**: 8790–8798.
27. Bodkin MJ, Goodfellow JM. Hydrophobic solvation in aqueous trifluoroethanol solution. *Biopolymers* 1996; **39**: 43–50.
28. Przybylski M, Glocker MO. Electrospray mass spectrometry of biomacromolecular complexes with noncovalent interactions — New analytical perspectives for supramolecular chemistrry and molecular recognition processes. *Angew. Chem. Int. Ed. Engl.* 1996; **35**: 807–826.
29. Li Y-T, Hsieh Y-L, Henion JD, Senko MW, McLafferty FW, Ganem B. Mass spectrometric studies on noncovalent dimers of leucine zipper peptides. *J. Am. Chem. Soc.* 1993; **115**: 8409–8413.
30. Marti DN, Jelesarov I, Bosshard HR. Interhelical ion pairing in coiled-coils: solution structure of a heterodimeric leucine zipper and determination of pK_a values of Glu side chains. *Biochemistry* 2000; **39**: 12 804–12 818.

